AN INVESTIGATION ON CORROSION INHIBITORS FOR STEEL IN ETHANOL FUEL BLEND

Nguyen Si Hoai Vu[1, 2], Vu Thi Hanh Thu[1], Do Chiem Tai[3], Nguyen Dang Nam[2, *]

[1]*Department of Physics & Engineering Physics, VNUHCM-University of Science, 227 Nguyen Van Cu Street, District 5, Ho Chi Minh City 700000*

[2]*Institute of Fundamental and Applied Sciences, Duy Tan University, 10C Tran Nhat Duat Street, District 1, Ho Chi Minh City 700000*

[3]*PetroVietnam University, 762 Cach Mang Thang Tam Street, Long Toan Ward, Ba Ria City 790000*

[*]Email: *nguyendangnam@dtu.edu.vn; namnd@pvu.edu.vn*

Received: 8 July 2018; Accepted for publication: 9 September 2018

ABSTRACT

Cerium (III) chloride ($CeCl_3$), sodium 4-hydroxycinnamate (Na(4-OHCin)), and cerium 4-hydroxycinnamate ($Ce(4\text{-}OHCin)_3$) have been successfully characterized as effective anodic, cathodic, and mixed inhibitors for steel in simulated ethanol fuel blend (SEFB) by electrochemical and surface analyses. Electrochemical and surface analyses indicate that good inhibition performances are due to the formation of protective layer as a result of adsorption between the metal and inhibitor components. In addition, the inhibition mechanism of each inhibitor is also suggested and discussed in detail.

Keywords: steel; ethanol fuel blend; corrosion inhibitor; electrochemistry, surface analysis.

1. INTRODUCTION

The acceptance that fossil fuels, particularly crude oil, significantly affect to human health and environment [1]. It is therefore a new energy source is required that could be an alternative to the fossil fuels. Among many ways, bio-gasoline could be a good choice due to its lower combustion energy and corresponding fuel economy. Furthermore, ethanol is becoming an excellent candidate as a popular fuel due to its renewable property and more environmentally friendly in comparison with gasoline [2]. It has been using as an engine fuel and fuel additive. Particularly, ethanol in fuel reduces harmful tailpipe emissions such as carbon monoxide, oxides of nitrogen, and others related to pollutants [3]. The processes of storage tanks for the finished product used a large carbon steel for the fuel grade ethanol producers. During these processes such as storage, production, and distribution, contaminants including water, acetic acid, and chloride, et al. could play a significant role since contaminants could be a cause of corrosion and stress corrosion cracking [4]. Therefore, the application of adsorption or protective layer

formation on the metal surface is to increase the corrosion resistance which plays a crucial role in minimizing the cost and reducing the toxic affect [5]. Particularly, inhibitors can mitigate the corrosion with no change of any producing processes but unfortunately, in practice, the selection and application of inhibitors are actually complicated since the corrosion environments in the storage of biogasoline are very variable. Therefore, it leads an important study for new, more efficient, and environmentally benign inhibitor systems during the storage of gasoline. In the present decades, leaf extracts were a good recommendation for inhibiting corrosion with high performance [6]. However, these complexes molecular could effect to the products and its refined processes pay for the high energy and cost. Second choice can be accounted for the novel chemical approaches to corrosion inhibition such as rare-earth compounds that perform a dramatic synergistically improved inhibition when these compounds were compared with their individual components [7]. Other choice is ionic liquid treatments to passivate reactive metal surfaces. Among these new technologies, a multifunctional inhibitor could provide superior inhibition than either of the individual components and other technology at the same level and condition. Particularly, rare earth organic compounds are complementary to the existing inhibitor expertise we currently have and will therefore be of great benefit in developing new systems for new application areas. Therefore, $CeCl_3$ and Na(4-OHCin) as the individual components and $Ce(4\text{-}OHCin)_3$ as a multifunctional inhibitor will be used and compared the inhibition characterizations for steel in ethanol fuel blend using advanced electrochemical and surface analysis techniques. In addition, inside of corrosion and inhibition is also considered and discussed within this work.

2. MATERIALS AND METHODS

The reagents used in this work include cerium chloride, trans 4-hydroxycinnamic acid, sodium chloride, and others were purchased from Sigma Aldrich with ≥99% pure and used without further purification. Na(4-OHCin) and $Ce(4\text{-}OHCin)_3$ were synthesized as such that was previously reported [8]. Na(4-OHCin), $CeCl_3$, and $Ce(4\text{-}OHCin)_3$ were dissolved in the simulated ethanol fuel blend contents are described previous work [6] and added slowly with stirring at 900 rpm and 38 ºC for 12 h making the final concentrations of 1800, 600, and 600 ppm of Na(4-OHCin), $CeCl_3$, and $Ce(4\text{-}OHCin)_3$, respectively. The steel coupons of 1.0 × 1.0 × 0.3 cm^3 used as working electrodes for the electrochemical tests were fabricated from steel sheet. These steel specimens were coolly mounted by a low viscosity epoxy system for producing 1 cm^2 of the exposed area. All specimens were finished by 1200-grit silicon carbide paper and then rinsed with deionized water and ethanol before running experiments. A standard three electrode system including a silver/silver chloride reference electrode, a titanium mesh counter electrode, and the working electrode was used for carrying out electrochemical experiments. The electrochemical tests were conducted using a VSP of BioLogic Scientific Instruments. All electrochemical tests were undertaken after 24 h of immersion in the simulated ethanol fuel blend as open circuit potential. The electrochemical impedance spectroscopy (EIS) test was conducted at 10 mV peak-to-peak amplitude of the sinusoidal perturbation and the frequency range from 10 kHz to 100 mHz. Potentiodynamic polarization (PD) tests were also carried out after 24 h of immersion in the simulated ethanol fuel blend at a rate of 0.166 mV/s from an initial potential of -250 mV (vs. E_{corr}) to a selected anodic potential at 300 $mV_{Ag/AgCl}$. The inhibition efficiency (η, %) was calculated by the following equations: $\eta = (1\text{-}i_{corr}/i^{o}_{corr})\times 100$, where i^{o}_{corr} and i_{corr} are the values of the corrosion current density without and with the inhibitor addition, respectively. In addition, the chemical species formed on the steel surfaces after 24 h

exposed time in the simulated ethanol fuel blend were characterized by scanning electron microscopy and attenuated total reflectance Fourier transform infrared spectroscopy.

3. RESULTS AND DISCUSSION

To study the protective layer formation and inhibition efficiency, potentiodynamic polarization measurements were carried out. Representative PD curves of the steels after 24 h immersion in SEFB without and with inhibitors are given in Fig. 1.

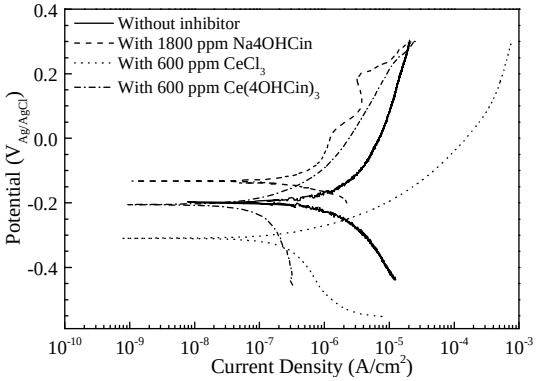

Figure 1. Potentiodynamic polarization curves of steel after 24 h immersion in simulated ethanol fuel blend without and with inhibitor addition.

The results indicated that formation of protective layer was observed on the specimens immersed in SEFB containing Na(4-OHCin) and $Ce(4\text{-}OHCin)_3$ compounds, whereas active behaviors were observed on the specimens immersed in SEFB without and with $CeCl_3$ addition. In the present study, i_{corr} values were reached by Tafel extrapolation methods. Where anodic and cathodic curves must be nearby linear and movable within ±100 mV from E_{corr}, they were extrapolated when these lines were intersected at E_{corr}. The experimental and analysis results indicated that steel immersed in SEFB without inhibitor additions behaved more active in comparing with steels immersed in SEFB with inhibitor additions due to the highest corrosion current density reached 2.2 $\mu A/cm^2$, whereas that values were 0.411, 0.273, and 0.204 $\mu A/cm^2$ for the specimens immersed in SEFB containing Na(4-OHCin), $CeCl_3$, and $Ce(4\text{-}OHCin)_3$, respectively. All corrosion parameters are given in Table 1. When Na(4-OHCin) and $CeCl_3$ were added to SEFB, a significant shift in E_{corr} was more positive and negative values, suggesting anodic and cathodic behaviors. These phenomena could affect to anodic and cathodic reactions of electrochemical processes, resulting in a strong shift of i_{corr} that make a decrease in corrosion rate.

When $Ce(4\text{-}OHCin)_3$ was added to SEFB, mixed inhibition was performed due to a strong shift in i_{corr} value and E_{corr} remained around that value of specimen immersed in SEFB without inhibitor additions. As shown in Fig. 1, the corrosion current density was strongly decreased when inhibitors were added to SEFB. Furthermore, the most effective inhibition was reached for specimen immersed in SEFB containing $Ce(4\text{-}OHCin)_3$. The anodic branches showed the formation of the protective film on specimens immersed in SEFB containing both Na(4-OHCin) and $Ce(4\text{-}OHCin)_3$ due to the remain low current densities from E_{corr} to final potential. However, a significant effect on the cathodic reactions was observed on specimen immersed in SEFB containing $CeCl_3$ due to the strong shift to negative potentials, resulting in a cathodic inhibition. In addition, it also showed that the cathodic polarization behavior was significantly increased

due to the cerium ion's precipitations to form the film on the specimen surface. Above phenomena could result in a decrease in the ion diffusion in the metallic surface that improved the surface's electrical resistance, indicating an improved corrosion resistance. The highest inhibition efficiency in Table 1 indicated the best inhibition performance of $Ce(4\text{-}OHCin)_3$ compound in comparison with other inhibitors under the same experimental conditions.

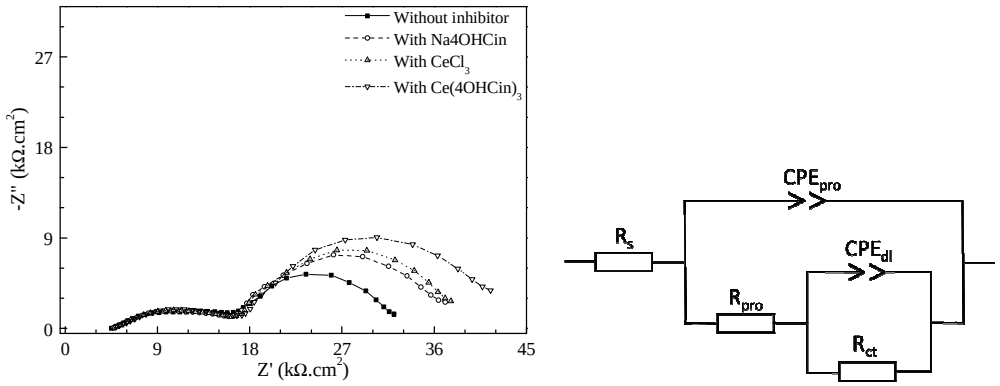

Figure 2. (a) Nyquist plots of steel after 24 h immersion in simulated ethanol fuel blend without and with inhibitor addition, and (d) an equivalent circuit for fitting the EIS data.

Table 1. Corrosion parameters obtained from the potentiodynamic polarization curves.

Concentration (ppm)	E_{corr} ($mV_{Ag/AgCl}$)	i_{corr} ($\mu A/cm^2$)	β_a (V/decade)	$-\beta_c$ (V/decade)	Inhibition efficiency (η %)
0	-198	2.200	315	295	-
Na4OHCin (1800)	-133	0.411	123	54	81.32
$CeCl_3$ (600)	-309	0.273	55	197	87.59
$Ce(4OHCin)_3$ (600)	-205	0.204	82	198	90.72

We can now begin to correlate the EIS data with the potentiodynamic polarization results. The EIS results measured at the rest potential in the form of Nyquist plots were displayed in Fig. 2(a). A depressed semicircular was performed in the Nyquist diagram could be due to the heterogeneity (surface roughness) of the specimen surfaces. In addition, an increase of the diameter of the semicircle and impedance values suggests the growth of a more capacitive film, indicating the formation and an increased coverage of protective film. It is obviously that the arc spectra are strongly dependent on the inhibitor. It is also evident that the EIS performed two capacitive arcs for all specimens, where the first capacitive arc correlates to rust when steel was immersed in SEFB without inhibitor addition, whereas that capacitive arc is attributed to the formation of the protective film for steel immersed in SEFB with inhibitor additions. It is important that the presence of surface films could hinder diffusion of ions, expressing two time constants in all impedance spectrums. The impedances at the medium and low frequency were significantly increased as a result of the increase of the film and charge transfer resistances, suggesting the barrier properties. The EIS results indicated that these studied inhibitors behave corrosion inhibition. Based on electrochemical and surface analysis, an equivalent circuit was simulated and derived for fitting EIS results to optimize the protective layer and charge transfer resistance parameters as well as CPE magnitudes. The equivalent circuits given in Fig. 2(b) were chosen for modeling the EIS data via the Zsimpwin Program. This equivalent circuit consists of R_s as the solution resistance, CPE1 and CPE2 as the constant phase elements of the protective film and double layers (CPE contains a CPE magnitude and an exponent (n)), R_{pro} and R_{ct} as the

protective film and charge transfer resistances, respectively. It is noticed that protective layer was replaced by rust for steel in uninhibited system. EIS data and above equivalent circuit were added to the Zsimpwin program for fitting the data. It could be observed that the investigated solution have not so good conductivity due to a high solution resistance performed in all results. Furthermore, the R_{pro} and R_{ct} values observed on inhibited system were higher than that for uninhibited system under the same experimental conditions. This should be attributed to the formation of the protective barrier films on the steel surfaces as observed and identified via PD and surface analysis. Higher R_{ct} value is important since R_{ct} correlates to the exchange current density of the metal/metal ions system, indicating better corrosion resistance. Furthermore, lower CPE magnitude values were also observed on inhibited system, suggesting an inhibition of the penetration of aggressive components in the electrolyte into the protective layers. Therefore, higher R_{pro} and R_{ct} values, as well as lower CPE magnitude values could be resulted in the entire surface being covered by a protective film that could reduce the pore density and the improvement of film compactness, and adhesion to the underlying surface. These phenomena could increase in coverage of the protective layer, resulting in higher inhibition of the corrosion process for $Ce(4\text{-}OHCin)_3$ compound.

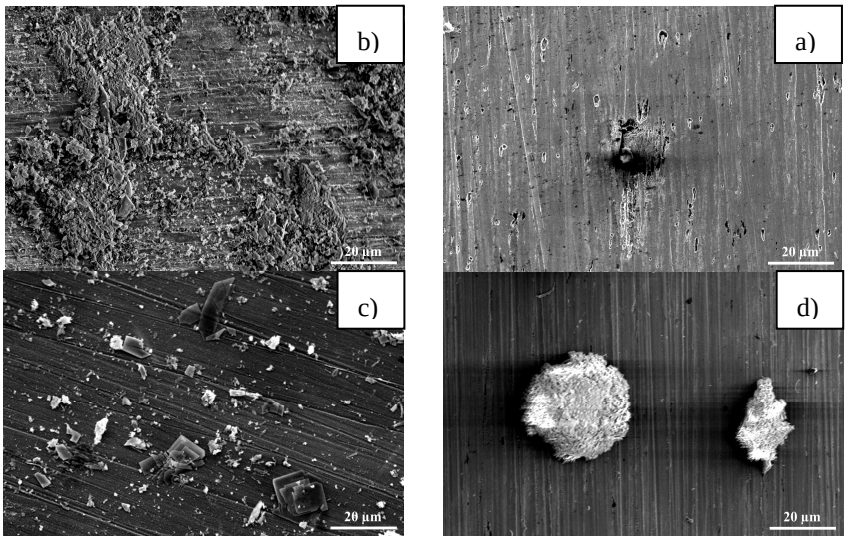

Figure 3. SEM images of steel surfaces after 24 h immersion in simulated ethanol fuel blend: (a) without inhibitor addition and with (b) 1800 ppm Na(4-OHCin), (c) 600 ppm $CeCl_3$, and (d) 600 ppm $Ce(4\text{-}OHCin)_3$.

Figure 3 presents the SEM images of steel surfaces after 24 h immersion in simulated ethanol fuel blend without and with inhibitor additions. It indicated that steel surface immersed in uninhibited SEFB showed an evident corrosion attack on the steel surface as shown in Fig. 3(a), whereas, less corrosion attack was showed on the steel surfaces immersed in inhibited systems, that indicated an uniform (Fig. 3(b) and non-uniform deposits (Fig. 3(c and d) formed on steel surfaces immersed in SEFB containing Na(4-OHCin), $CeCl_3$, and $Ce(4\text{-}OHCin)_3$, respectively. Although uniform film formed on steel surface immersed in SEFB containing Na(4-OHCin), there are still corrosion attack due to disadvantage of anodic inhibitor performed in electrochemical results. Non-uniform deposits and less corrosion attack were showed on steel surfaces immersed in SEFB containing $CeCl_3$ and $Ce(4\text{-}OHCin)_3$ acted as cathodic and mixed corrosion inhibitor evidently performed in above electrochemical results. Furthermore, mixed

inhibitor, Ce(4-OHCin)$_3$, expressed advantages of both anodic and cathodic inhibitors, resulting in a multifunction of behaviors of both anodic and cathodic inhibitors. The results also indicated crystalline particles formed on steel surface immersed in SEFB containing $CeCl_3$ and Ce(4-OHCin)$_3$, that could be resulted of selective deposits of inhibitor components. Other places could be formed a thinner surface film away from the selectively deposited particles, resulting in a less corrosion attack on steel surfaces immersed in those systems.

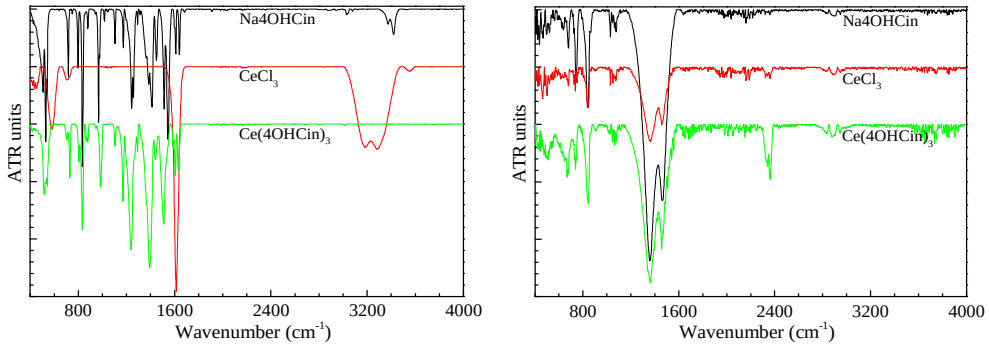

Figure 4. ATR-FTIR analysis of (a) Na(4-OHCin), $CeCl_3$, and Ce(4-OHCin)$_3$ powders and (b) steel surfaces 24 h immersion in simulated ethanol fuel blend with inhibitor addition.

Figure 4(a) presents the ATR-FTIR results of Na(4-OHCin), $CeCl_3$, and Ce(4-OHCin)$_3$ powders as raw corrosion inhibitor materials. It indicated that only signals of Ce-Cl and water molecule peaks were observed on the $CeCl_3$ materials. The water molecule peaks are attributed to the hydration of $CeCl_3$. The results of Na(4-OHCin) and Ce(4-OHCin)$_3$ present $\nu(C=C)_{propenyl}$ bands assigned for the Na and Ce^{III} 4-hydroxycinnamate complexes around 1630 cm^{-1}. Other $\nu_{as}(CO_2)$ and $\nu_s(CO_2)$ peaks could be assigned around 1510 and 1410 cm^{-1}, respectively. It is noticed that a small shift of these peaks observed on Na(4-OHCin) and Ce(4-OHCin)$_3$ powders could be contributed to the different bonds between Na and Ce^{III} with 4-hydroxycinnamate group. These ATR-FTIR results were agreed with previous works [8]. Fig. 4(b) showed the representative ATR-FTIR results of steel surfaces after 24 h immersion in SEFB containing inhibitors. All results indicated the presence of the hydrated iron oxide/hydroxide on steel surfaces assigned at the absorption bands from 1000 and 1200 cm^{-1}. Furthermore, the steel surface immersed in SEFB containing Na(4-OHCin) and Ce(4-OHCin)$_3$ showed C=C vibration from the propenyl group around the bands at 1640 cm^{-1}, $\nu_{as}(COO^-)$ and $\nu_s(COO^-)$ absorption peaks around 1500 and 1400 cm^{-1}, respectively. Particularly, these peaks were slightly shifted in comparison with that of raw materials, indicating the adsorption of inhibitor species on the surfaces and should not like a physical accumulation of inhibitor onto the substrate surfaces. These peaks observed on the steel surface immersed in SEFB containing $CeCl_3$ can be attributed to the basis of cerium carbonate spectra.

In this study, the initial corrosion could concentrate to the imperfect location on the steel surface, promoting the metal dissolution due to the availably aggressive ions in the simulated ethanol fuel blend. When inhibitors had not been added to solution, corrosion could be widely developed, resulting in the evident corrosion attack on the steel surface and higher corrosion rate showed in the electrochemical results. Fortunately, when steel was immersed on SEFB containing inhibitors, the 4-hydroxycinnamate species could be coordinated with positive ions initially generated at the active sites. This phenomena will be continued to coordinate with new

positive ions due to the availability of aggressive ions and 4-hydroxycinnamate species in SEFB containing Na(4-OHCin), resulting in entire surface film (continuous or uniform protective film) formation due to anodic inhibition activity of 4-hydroxycinnamate species. For steel immersed in SEFB containing $CeCl_3$, cerium ions will be hydrolyzed at the cathode of localized electrochemical reactions to precipitate the cerium metal hydroxide and iron oxide/hydroxide species, resulting in a heterogeneous protective surface film in Fig. 3(c). Above phenomenon will be resulted in selective adsorption to form the inhibitor rich particles on the surface as shown in Figs. 3(d) and 4(b) for steel immersed in SEFB containing $Ce(4\text{-}OHCin)_3$. In addition, cerium ions will be hydrolyzed at the cathode of electrochemical reactions to form the precipitation of rare earth metal and iron oxide/hydroxide species to form thin film beside particles. Higher inhibition performance of $Ce(4\text{-}OHCin)_3$ compound could be attributed to the combination of anodic and cathodic multifunction properties of $CeCl_3$ and Na(4-OHCin), that performed as cathodic and anodic inhibitors, respectively. Therefore, a difference of inhibition performances and surface morphologies was achieved for steel in SEFB.

4. CONCLUSIONS

It was evident that the addition of these inhibitors to the simulated ethanol fuel blend has significantly showed their effectiveness in an improved corrosion resistance of steel. Interestingly, Na(4-OHCin) and $CeCl_3$ referred acting as the anodic and cathodic inhibitors, respectively. Whereas $Ce(4\text{-}OHCin)_3$ compound showed the mixed anodic-cathodic behavior. Higher protective and charge transfer resistances have been achieved for contributing an important role in improving the corrosion resistance of steel in the simulated ethanol fuel blend. Surface analyses indicated that these compounds formed a protective film on the steel surface, contributing to the presence of cerium, iron oxide/hydroxide and 4-hydroxycinnamate components on the protective film. By looking at the benefits of these compounds, this study classified the types of corrosion inhibitor and supplied a promising way to the expansion of corrosion inhibitors for steel as an application for biogasoline's storage.

Acknowledgement. This research is funded by Ho Chi Minh City Department of Science and Technology under grant code 136/2017/H--SKHCN (780/Q--SKHCN). The authors are also grateful for the support of PetroVietnam University.

REFERENCES

1. Barbir F., Veziroglu T. N., Plas H. J. - Environmental damage due to fossil fuels use, Int. J. Hydrogen Energy **15** (1990) 739-749.
2. Jeong J., Jeon H., Ko K. - Production of anhydrous ethanol using various PSA (Pressure Swing Adsorption) processes in pilot plant, Renewable Energy **42** (2012) 41-45.
3. Madronich S. - Atmospheric chemistry: Ethanol and ozone, Nat. Geosci. **7** (2014) 395-397.
4. Sowards J. W., Weeks T. S. - The influence of simulated fuel-grade ethanol on fatigue crack propagation in pipeline and storage-tank steels, Corros. Sci. **75** (2013) 415-425.
5. Lateef H. M. A. E., Riya M. A. A., Tantawy A. H. – Empirical and quantum chemical studies on the corrosion inhibition performance of some novel synthesized cationic gemini surfactants on carbon steel pipelines in acid pickling, Corros. Sci. **108** (2016) 94-110.
6. Vu N. S. H., Hien P. V., Man T. V., Thu V. T. H, Tri M. D., Nam N. D. - A study on corrosion inhibitor for mild steel in ethanol fuel blend, Materials **11** (2018) 59.

7. Seter M., Thomson M. J., Chong A., MacFarlane D. R., Forsyth M. - Cetrimonium nalidixate as a multifunctional inhibitor to combat biofilm formation and microbiologically influenced corrosion, Aust. J. Chem. **66** (2013) 921-929.
8. Deacon G. B., Forsyth M. - Synthesis and characterisation of rare earth complexes supported by para-substituted cinnamate ligands, Z. Anorg. Allg. Chem. **635** (2009) 833-839.